

Exploring R_D , R_{D^*} and $R_{J/\Psi}$ anomalies

Rupak Dutta*

National Institute of Technology Silchar, Silchar 788010, India

Deviations from the standard model predictions have been reported in various observables concerned with the lepton flavor universality. At present, the deviation of the measured values of R_D and R_{D^*} from the standard model expectation is exceeded by 2.3σ and 3.4σ , respectively. Very recently LHCb has measured the ratio of branching ratio $R_{J/\Psi} = \mathcal{B}(B_c \rightarrow J/\Psi \tau \nu) / \mathcal{B}(B_c \rightarrow J/\Psi l \nu)$, where $l \in (e, \mu)$, to be $0.71 \pm 0.17 \pm 0.18$ which is at more than 2σ away from the standard model prediction. We investigate the anomalies in R_D , R_{D^*} , and $R_{J/\Psi}$ using a model independent framework with minimal number of new physics couplings. We find various new physics models that can explain these anomalies within 1σ .

PACS numbers: 14.40.Nd, 13.20.He, 13.20.-v

I. INTRODUCTION

Lepton flavor universality violation has been the center of attention due to the long standing anomalies that persisted in the ratio of branching ratios R_D and R_{D^*} , where

$$R_{D^{(*)}} = \frac{\mathcal{B}(B \rightarrow D^{(*)} \tau \nu)}{\mathcal{B}(B \rightarrow D^{(*)} l \nu)}, \quad l \in (e, \mu). \quad (1)$$

Unlike the individual branching ratio of these decay modes, R_D and R_{D^*} do not suffer from the uncertainties coming from the Cabbibo-Kobayashi-Mashakawa (CKM) matrix elements and the meson to meson form factors. The dependency on the CKM matrix elements exactly cancels in these ratios. Similarly, the uncertainties due to the form factors also largely cancel in these ratios and a clean prediction of R_D and R_{D^*} can be made within the standard model (SM). Hence, any deviation from the SM prediction would clearly indicate the presence of new physics (NP). At present, combining the results of R_D and R_{D^*} measured by various experiments such as BABAR [1, 2], BELLE [3–5], and LHCb [6, 7], i.e. $R_D = 0.407 \pm 0.039 \pm 0.024$ and $R_{D^*} = 0.304 \pm 0.013 \pm 0.007$ exceed the SM predictions by 2.3σ and 3.4σ , respectively. Again, including the $R_D - R_{D^*}$ correlation, the discrepancy with SM prediction [8–12] currently stands at about 4.1σ [13]. Recently, LHCb [14, 15] has measured the value of the ratio of branching ratio

$$R_{J/\Psi} = \frac{\mathcal{B}(B_c \rightarrow J/\Psi \tau \nu)}{\mathcal{B}(B_c \rightarrow J/\Psi l \nu)} = 0.71 \pm 0.17 \pm 0.18, \quad (2)$$

where l is either an electron or muon, which is at more than 2σ away from the standard model (SM) prediction [16, 17]. In Ref. [5], the τ polarization fraction in $B \rightarrow D^* \tau \nu$ decays has also been measured by BELLE Collaboration and it is reported to be $P_\tau^{D^*} = -0.38 \pm 0.51_{-0.16}^{+0.21}$. All these measurements indicate an upward deviation from the SM expectation.

Various model-independent and model-dependent [18–41] approaches have been carried out to explore NP effects in R_D and R_{D^*} . Very recently, NP effects on $B_c \rightarrow J/\Psi \tau \nu$ decays has also been studied by various authors [17, 42, 43]. In view of the new measurement of $R_{J/\Psi}$ made by LHCb, we investigate R_D , R_{D^*} , and $R_{J/\Psi}$ anomalies within a model independent framework with minimal number of NP couplings. We use the most general effective Lagrangian in the presence of NP which is valid at renormalization scale $\mu = m_b$ and seek to find the minimal number of NP couplings that best fit the data. We have considered total 55 NP scenarios based on NP contributions from single operators as well as from two different operators and try to find the scenario that best explains R_D , R_{D^*} , and $R_{J/\Psi}$ anomalies. Although this is not entirely a new idea, most efforts at explaining these anomalies consider only a subset of these 55 NP structures. We do not propose any NP model that can generate such NP structures in particular. Rather we study it from a purely phenomenological point of view. It was shown in Ref. [38] that lifetime of B_c meson

*Electronic address: rupak@phy.nits.ac.in

put a severe constraint on scalar type NP interactions. Based on various SM calculations [44–46], it was inferred that $\mathcal{B}(B_c \rightarrow \tau\nu) \leq 5\%$ is necessary to comply with the current world average of the B_c lifetime. However, the constraint can be relaxed up to 30% depending on the value of the total decay width of B_c meson that is used as input for the SM calculation of various partonic transitions. Very recently, in Ref. [47], a more significant bound of $\mathcal{B}(B_c \rightarrow \tau\nu) \leq 10\%$ was obtained by taking the LEP data at the Z peak. Our analysis also takes into account the indirect constraint coming from $\mathcal{B}(B_c \rightarrow \tau\nu)$ to rule out various NP scenarios. We, however, have not included the measured value of P_τ^{D*} reported by Belle in our fitting method since the uncertainties associated with it is rather large.

The paper is organized as follows. In section. II, we present the most general effective weak Lagrangian for the $b \rightarrow c\tau\nu$ quark level transitions in the presence of NP valid at renormalization scale $\mu = m_b$. We also present all the relevant formulas pertinent for our analysis. The results of our analysis are reported in section. III. We conclude with a brief summary of our results in section. IV.

II. THEORY FRAMEWORK

We begin with the most general effective Lagrangian for the $b \rightarrow c\ell\nu$ quark level transitions in the presence of NP. That is [48, 49]

$$\begin{aligned} \mathcal{L}_{\text{eff}} = & -\frac{4G_F}{\sqrt{2}} V_{cb} \left\{ (1 + V_L) \bar{\ell}_L \gamma_\mu \nu_L \bar{c}_L \gamma^\mu b_L + V_R \bar{\ell}_L \gamma_\mu \nu_L \bar{c}_R \gamma^\mu b_R + \tilde{V}_L \bar{\ell}_R \gamma_\mu \nu_R \bar{c}_L \gamma^\mu b_L + \tilde{V}_R \bar{\ell}_R \gamma_\mu \nu_R \bar{c}_R \gamma^\mu b_R + \right. \\ & S_L \bar{\ell}_R \nu_L \bar{c}_R b_L + S_R \bar{\ell}_R \nu_L \bar{c}_L b_R + \tilde{S}_L \bar{\ell}_L \nu_R \bar{c}_R b_L + \tilde{S}_R \bar{\ell}_L \nu_R \bar{c}_L b_R + T_L \bar{\ell}_R \sigma_{\mu\nu} \nu_L \bar{q}'_R \sigma^{\mu\nu} b_L + \\ & \left. \tilde{T}_L \bar{\ell}_L \sigma_{\mu\nu} \nu_R \bar{q}'_L \sigma^{\mu\nu} b_R \right\} + \text{H.c.}, \end{aligned} \quad (3)$$

where $(V_L, V_R, S_L, S_R, T_L)$ represents NP couplings that involve left handed neutrino interactions and $(\tilde{V}_L, \tilde{V}_R, \tilde{S}_L, \tilde{S}_R, \tilde{T}_L)$ represents NP couplings that involve right handed neutrino interactions. We consider all the NP couplings to be real. In the presence of such NP, the three body differential branching ratios for $B_q \rightarrow (P, V)\ell\nu$ decays, where $P(V)$ represents pseudoscalar (vector) meson, can be written as [29, 32, 42]

$$\frac{d\Gamma^P}{dq^2}(+) = \frac{8N|\vec{p}_P|}{3} \left\{ \frac{m_l^2}{q^2} \left[\tilde{H}_{T0}^2 + \frac{1}{2} H_{0T}^2 + \frac{3}{2} H_{tS}^2 \right] \right\}, \quad \frac{d\Gamma^P}{dq^2}(-) = \frac{8N|\vec{p}_P|}{3} \left\{ \frac{m_l^2}{q^2} \left[H_{T0}^2 + \frac{1}{2} \tilde{H}_{0T}^2 + \frac{3}{2} \tilde{H}_{tS}^2 \right] \right\}, \quad (4)$$

where

$$\begin{aligned} H_0 &= \frac{2m_{B_q}|\vec{p}_P|}{\sqrt{q^2}} F_+(q^2), & H_t &= \frac{m_{B_q}^2 - m_P^2}{\sqrt{q^2}} F_0(q^2), & H_S &= \frac{m_{B_q}^2 - m_P^2}{m_b(\mu) - m_c(\mu)} F_0(q^2), & H_T &= \frac{8m_{B_q}|\vec{p}_P|}{m_{B_q} + m_P} F_T, \\ H_{T0} &= H_T T_L + \frac{\sqrt{q^2}}{m_l} H_0 G_V, & \tilde{H}_{T0} &= H_T \tilde{T}_L + \frac{\sqrt{q^2}}{m_l} H_0 \tilde{G}_V, & H_{0T} &= H_0 G_V + \frac{\sqrt{q^2}}{m_l} H_T T_L, \\ \tilde{H}_{0T} &= H_0 \tilde{G}_V + \frac{\sqrt{q^2}}{m_l} H_T \tilde{T}_L, & H_{tS} &= H_t G_V + \frac{\sqrt{q^2}}{m_l} H_S G_S, & \tilde{H}_{tS} &= H_t \tilde{G}_V + \frac{\sqrt{q^2}}{m_l} H_S \tilde{G}_S. \end{aligned} \quad (5)$$

Similarly

$$\frac{d\Gamma^V}{dq^2}(+) = \frac{8N|\vec{p}_P|}{3} \left\{ \frac{m_l^2}{q^2} \left[\tilde{\mathcal{A}}_{TAV}^2 + \frac{1}{2} \mathcal{A}_{AVT}^2 + \frac{3}{2} \mathcal{A}_{tP}^2 \right] \right\}, \quad \frac{d\Gamma^V}{dq^2}(-) = \frac{8N|\vec{p}_P|}{3} \left\{ \frac{m_l^2}{q^2} \left[\mathcal{A}_{TAV}^2 + \frac{1}{2} \tilde{\mathcal{A}}_{AVT}^2 + \frac{3}{2} \tilde{\mathcal{A}}_{tP}^2 \right] \right\}, \quad (6)$$

where

$$\begin{aligned} \mathcal{A}_{TAV}^2 &= \left(\mathcal{A}_{T_0} T_L + \frac{\sqrt{q^2}}{m_l} \mathcal{A}_0 G_A \right)^2 + \left(\mathcal{A}_{T_2} T_L + \frac{\sqrt{q^2}}{m_l} \mathcal{A}_{||} G_A \right)^2 + \left(\mathcal{A}_{T_1} T_L + \frac{\sqrt{q^2}}{m_l} \mathcal{A}_\perp G_V \right)^2, \\ \tilde{\mathcal{A}}_{TAV}^2 &= \left(\mathcal{A}_{T_0} \tilde{T}_L + \frac{\sqrt{q^2}}{m_l} \mathcal{A}_0 \tilde{G}_A \right)^2 + \left(\mathcal{A}_{T_2} \tilde{T}_L + \frac{\sqrt{q^2}}{m_l} \mathcal{A}_{||} \tilde{G}_A \right)^2 + \left(\mathcal{A}_{T_1} \tilde{T}_L + \frac{\sqrt{q^2}}{m_l} \mathcal{A}_\perp \tilde{G}_V \right)^2, \\ \mathcal{A}_{AVT}^2 &= \left(\mathcal{A}_0 G_A + \frac{\sqrt{q^2}}{m_l} \mathcal{A}_{T_0} T_L \right)^2 + \left(\mathcal{A}_{||} G_A + \frac{\sqrt{q^2}}{m_l} \mathcal{A}_{T_2} T_L \right)^2 + \left(\mathcal{A}_\perp G_V + \frac{\sqrt{q^2}}{m_l} \mathcal{A}_{T_1} T_L \right)^2, \\ \tilde{\mathcal{A}}_{AVT}^2 &= \left(\mathcal{A}_0 \tilde{G}_A + \frac{\sqrt{q^2}}{m_l} \mathcal{A}_{T_0} \tilde{T}_L \right)^2 + \left(\mathcal{A}_{||} \tilde{G}_A + \frac{\sqrt{q^2}}{m_l} \mathcal{A}_{T_2} \tilde{T}_L \right)^2 + \left(\mathcal{A}_\perp \tilde{G}_V + \frac{\sqrt{q^2}}{m_l} \mathcal{A}_{T_1} \tilde{T}_L \right)^2, \\ \mathcal{A}_{tP} &= \mathcal{A}_t G_A + \frac{\sqrt{q^2}}{m_l} \mathcal{A}_P G_P, & \tilde{\mathcal{A}}_{tP} &= \mathcal{A}_t \tilde{G}_A + \frac{\sqrt{q^2}}{m_l} \mathcal{A}_P \tilde{G}_P \end{aligned} \quad (7)$$

and

$$\begin{aligned}
\mathcal{A}_{\parallel} &= \frac{2(m_{B_q} + m_V)A_1(q^2)}{\sqrt{2}}, & \mathcal{A}_{\perp} &= -\frac{4m_{B_q}V(q^2)|\vec{p}_V|}{\sqrt{2}(m_{B_q} + m_V)}, & \mathcal{A}_{T_1} &= -\frac{8\sqrt{2}m_{B_q}|\vec{p}_V|}{\sqrt{q^2}}T_1, \\
\mathcal{A}_t &= \frac{2m_{B_q}|\vec{p}_V|A_0(q^2)}{\sqrt{q^2}}, & \mathcal{A}_P &= -\frac{2m_{B_q}|\vec{p}_V|A_0(q^2)}{(m_b(\mu) + m_c(\mu))}, & \mathcal{A}_{T_2} &= -\frac{4\sqrt{2}(m_{B_q}^2 - m_V^2)}{\sqrt{q^2}}T_2, \\
\mathcal{A}_0 &= \frac{1}{2m_V\sqrt{q^2}}\left[\left(m_{B_q}^2 - m_V^2 - q^2\right)(m_{B_q} + m_V)A_1(q^2) - \frac{4M_B^2|\vec{p}_V|^2}{m_{B_q} + m_V}A_2(q^2)\right], \\
\mathcal{A}_{T_0} &= \frac{2}{m_V}\left[-\left(m_{B_q}^2 + 3m_V^2 - q^2\right)T_2(q^2) + \frac{2m_{B_q}|\vec{p}_V|}{m_{B_q}^2 - m_V^2}T_3(q^2)\right].
\end{aligned} \tag{8}$$

Here we denote $G_V = 1 + V_L + V_R$, $G_A = 1 + V_L - V_R$, $G_S = S_L + S_R$, $G_P = S_L - S_R$, $\tilde{G}_V = \tilde{V}_L + \tilde{V}_R$, $\tilde{G}_A = \tilde{V}_L - \tilde{V}_R$, $\tilde{G}_S = \tilde{S}_L + \tilde{S}_R$, and $\tilde{G}_P = \tilde{S}_L - \tilde{S}_R$. Again, $|\vec{p}_{P(V)}| = \sqrt{\lambda(m_{B_q}^2, m_{P(V)}^2, q^2)}/2m_{B_q}$ denotes the three momentum vector of the outgoing meson. The ratio of branching ratios and τ polarization fractions for these decay modes are

$$R_M = \frac{\mathcal{B}(B_q \rightarrow M\tau\nu)}{\mathcal{B}(B_q \rightarrow Ml\nu)}, \quad P_{\tau}^M = \frac{\Gamma^M(+)-\Gamma^M(-)}{\Gamma^M(+)+\Gamma^M(-)}, \tag{9}$$

where, l is either an electron or a muon and B_q is either a B meson or a B_c meson. Similarly, M refers to the outgoing pseudoscalar or vector meson. Again, $\Gamma(+)$ and $\Gamma(-)$ denote the decay widths of positive and negative helicity τ lepton, respectively.

III. NUMERICAL ANALYSES

For the numerical estimates of all the observables we first report all the input parameters. For the quark, lepton, and meson masses, we use $m_b(m_b) = 4.18$ GeV, $m_c(m_b) = 0.91$ GeV, $m_e = 0.510998928 \times 10^{-3}$ GeV, $m_{\mu} = 0.10565837151$ GeV, $m_{\tau} = 1.77682$ GeV, $m_{J/\Psi} = 3.0969$ GeV, $m_{B^-} = 5.27931$ GeV, $m_{B_c} = 6.2751$ GeV, $m_{D^0} = 1.86483$ GeV, and $m_{D^{*0}} = 2.00685$ GeV [50]. Similarly, for the mean lifetime of B^- and B_c meson, we use $\tau_{B^-} = 1.638 \times 10^{-12}$ s and $\tau_{B_c} = 0.507 \times 10^{-12}$ s [50]. We use $f_{B_c} = 0.434(0.015)$ GeV from Ref. [51]. The value of CKM matrix element is taken to be $V_{cb} = 0.0409(0.0011)$ [50]. The uncertainty associated with f_{B_c} and V_{cb} are indicated by the number in parentheses.

In order to compute the branching fractions and other observables, we need information on various hadronic form factors that parametrizes the hadronic matrix elements of vector, axial vector, scalar, pseudoscalar, and tensor currents between two mesons. For the $B_c \rightarrow J/\Psi$ hadronic form factors, we follow ref. [16]. The relevant formula for $V(q^2)$, $A_0(q^2)$, $A_1(q^2)$, and $A_2(q^2)$ pertinent for our discussion, taken from ref. [16] is

$$F(q^2) = F(0) \exp\left[aq^2 + b(q^2)^2\right], \tag{10}$$

where F stands for the form factors V , A_0 , A_1 , and A_2 and a , b are the fitted parameters. The numerical values of $B_c \rightarrow J/\Psi$ form factors at $q^2 = 0$ and their fitted parameters a and b , calculated in perturbative QCD (PQCD) approach, are collected from ref. [16]. Similarly for the $B_c \rightarrow J/\Psi$ tensor form factors, we follow Ref. [42]. The relevant formulas pertinent for our numerical computation are

$$\begin{aligned}
T_1(q^2) &= \frac{m_b + m_c}{m_{B_c} + m_{J/\Psi}}V(q^2), & T_2(q^2) &= \frac{m_b - m_c}{m_{B_c} - m_{J/\Psi}}A_1(q^2), \\
T_3(q^2) &= -\frac{m_b - m_c}{q^2}\left[m_{B_c}\left(A_1(q^2) - A_2(q^2)\right) + m_{J/\Psi}\left(A_2(q^2) + A_1(q^2) - 2A_0(q^2)\right)\right].
\end{aligned} \tag{11}$$

A preliminary lattice calculation of $B_c \rightarrow J/\Psi$ transition form factors is reported in Ref. [52, 53].

The $B \rightarrow D$ transition form factors $F_0(q^2)$ and $F_+(q^2)$, calculated using lattice QCD techniques, are collected from Ref. [8]. For the tensor form factor $F_T(q^2)$, we use Ref. [54]. That is

$$F_T(q^2) = \frac{0.69}{\left(1 - \frac{q^2}{6.4^2}\right)\left(1 - 0.56\frac{q^2}{6.4^2}\right)} \tag{12}$$

Similarly, for $B \rightarrow D^*$ form factors, we follow the heavy quark effective theory (HQET) approach of Ref. [55]. We refer to Ref. [55] for all the relevant equations.

We first perform a χ^2 test to measure the disagreement of SM with the data. The χ^2 is defined as

$$\chi^2 = \sum_i \frac{(\mathcal{O}_i^{\text{th}} - \mathcal{O}_i^{\text{exp}})^2}{(\Delta \mathcal{O}_i^{\text{exp}})^2}, \quad (13)$$

where $\mathcal{O}_i^{\text{exp}}$ represents the measured central value of the observables and $\Delta \mathcal{O}_i^{\text{exp}}$ represents corresponding 1σ uncertainty. Similarly, $\mathcal{O}_i^{\text{th}}$ represents the theoretical prediction of the observables. We include a total of three measurements for the evaluation of χ^2 , namely, R_D , R_{D^*} , and $R_{J/\Psi}$. We have not included $P_\tau^{D^*}$ in our fit as the error associated with it is rather large. We have found $\chi_{\text{min}}^2 = 16.3$ in the SM. The χ_{min}^2 in the SM is obtained by performing a random scan of all the theory input parameters such as CKM matrix elements, meson decay constant, and meson to meson form factors within 1σ of their central values. The corresponding best estimates for all the observables are listed in Table. I.

Let us now evaluate χ_{min}^2 for various NP scenarios. First we consider that NP contributions are coming from an operator characterized by a single NP Wilson Coefficient (WC). We have considered total 10 such NP scenarios that involve left handed as well as right handed neutrino interactions. The χ_{min}^2 obtained in each scenario and the corresponding best estimates of all the observables are listed in Table. I. We observe that we obtain the best fit to the data with \tilde{T}_L NP coupling which corresponds to $\chi_{\text{min}}^2 = 1.7$ followed by V_L , \tilde{V}_L , and \tilde{V}_R with $\chi_{\text{min}}^2 = 2.1$ each. The branching ratio of $B_c \rightarrow \tau\nu$ obtained in each of these scenarios is consistent with $\mathcal{B}(B_c \rightarrow \tau\nu) \leq 5\%$ obtained in the SM. With \tilde{T}_L NP coupling, although the the best estimates of R_{D^*} and $R_{J/\Psi}$ lie inside the 1σ experimental range, the best estimate of R_D , however, lies outside 1σ of the experimental value. Similarly, with V_L and $\tilde{V}_{(L,R)}$ NP couplings although, the best estimates of R_D and R_{D^*} lie inside the 1σ experimental range, the best estimate of $R_{J/\Psi}$, however, lies outside 1σ of the experimental value. We show in Fig. 1 the 95% CL (blue band) allowed ranges in $(R_D, P_\tau^{D^*})$,

Coefficients	Best fit value	R_D	R_{D^*}	$R_{J/\Psi}$	$P_\tau^{D^*}$	$\mathcal{B}(B_c \rightarrow \tau\nu)\%$	χ_{min}^2
SM		0.334	0.255	0.291	-0.501	2.3	16.3
V_L	-2.11	0.398	0.307	0.356	-0.494	2.9	2.1
V_R	-0.09	0.276	0.295	0.345	-0.496	2.5	10.7
S_L	-1.51	0.365	0.330	0.418	-0.140	121.5	5.2
S_R	0.31	0.427	0.266	0.308	-0.431	12.1	9.6
\tilde{V}_L	0.48	0.398	0.309	0.367	-0.311	2.7	2.1
\tilde{V}_R	0.48	0.398	0.309	0.367	-0.311	2.7	2.1
\tilde{S}_L	0.73	0.432	0.262	0.302	-0.513	23.2	11.2
\tilde{S}_R	0.73	0.432	0.262	0.302	-0.513	23.2	11.2
T_L	-0.08	0.309	0.302	0.457	-0.467	2.0	5.6
\tilde{T}_L	0.27	0.352	0.305	0.585	-0.412	2.3	1.7

TABLE I: Best estimates of R_D , R_{D^*} , $R_{J/\Psi}$, $P_\tau^{D^*}$, and $\mathcal{B}(B_c \rightarrow \tau\nu)$ within the SM and within various NP scenarios.

$(R_{D^*}, P_\tau^{D^*})$, and $(R_{J/\Psi}, P_\tau^{J/\Psi})$ for NP scenarios with V_L , \tilde{V}_L , and \tilde{T}_L NP couplings. We observe that, although, V_L and \tilde{V}_L NP couplings can simultaneously explain the anomalies present in R_D and R_{D^*} , these couplings, however, can not accommodate the $R_{J/\Psi}$ data within 1σ . We note that with \tilde{T}_L NP coupling, the range obtained for $R_{J/\Psi}$ lies within the 1σ range of $R_{J/\Psi}$ data. However with \tilde{T}_L NP coupling, the range obtained for R_D lies outside the 1σ experimental range. Again, we want to emphasise that the range in τ polarization fraction $P_\tau^{D^*}$ for each scenarios lies inside the 1σ allowed range reported by Belle Collaboration. However, with \tilde{T}_L and \tilde{V}_L NP couplings, the central value lies inside the 95% (blue) CL allowed bands. We notice that with V_L NP coupling, the central value of $P_\tau^{D^*}$ reported by Belle Collaboration lies much above the range obtained in this scenario. However, the uncertainty associated with $P_\tau^{D^*}$ is rather large. Precise determination of this parameter in the future will play a crucial role in identifying the exact nature of NP.

Now let us consider that NP contributions are coming from two different operators characterized by two NP WC. We consider total 45 such NP scenarios. In Table. II, we show the best estimates of R_D , R_{D^*} , $R_{J/\Psi}$, $P_\tau^{D^*}$ and $\mathcal{B}(B_c \rightarrow \tau\nu)$ for each of these scenarios. We find that there are various NP scenarios that can simultaneously explain R_D , R_{D^*} , and $R_{J/\Psi}$ anomalies. We notice that with (V_R, \tilde{T}_L) NP couplings we obtain the best fit with the data with $\chi_{\text{min}}^2 = 0.43 \times 10^{-2}$ followed by $(\tilde{V}_R, \tilde{T}_L)$, (S_R, \tilde{T}_L) , and $(\tilde{V}_L, \tilde{T}_L)$ NP couplings with $\chi_{\text{min}}^2 = 0.013, 0.026, \text{ and } 0.11$, respectively. However, with (S_R, \tilde{T}_L) NP couplings, the best estimates of $\mathcal{B}(B_c \rightarrow \tau\nu) = 80.6\%$ is much above the

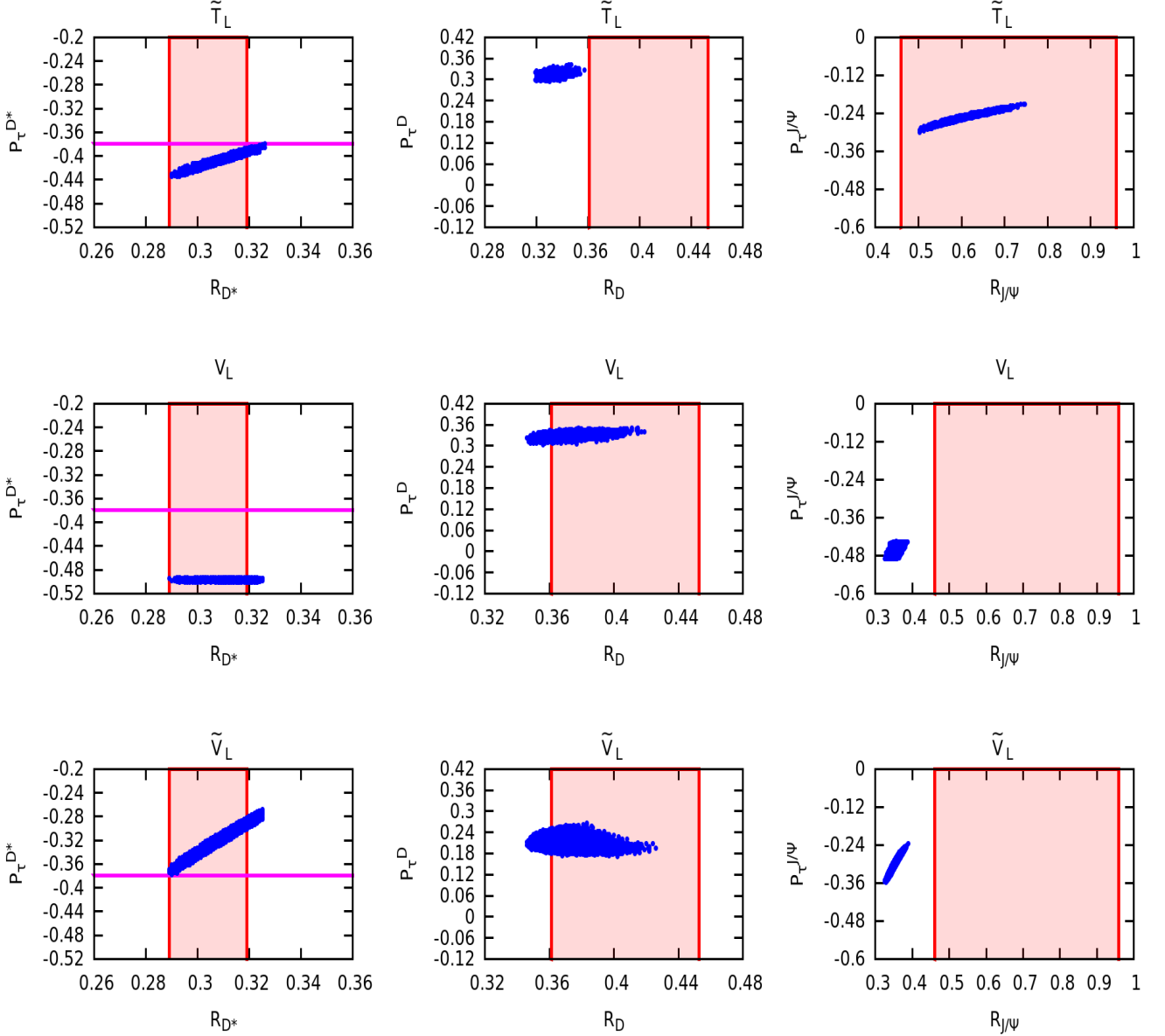


FIG. 1: The allowed ranges in (R_D, P_τ^D) , $(R_{D^*}, P_\tau^{D^*})$, and $(R_{J/\Psi}, P_\tau^{J/\Psi})$ at 95% CL are shown with blue bands. The experimental 1σ range of R_D , R_{D^*} , and $R_{J/\Psi}$ are shown with light red bands. The horizontal line in the leftmost panel represents the central value of $P_\tau^{D^*}$ reported by BELLE.

upper bound of $\mathcal{B}(B_c \rightarrow \tau\nu) \leq 30\%$ estimated in the SM. Hence although, we get a much better fit with this NP structure, (S_R, \tilde{T}_L) NP couplings can not accommodate the $B_c \rightarrow \tau\nu$ data.

We show in Fig. 2 the allowed range in (V_R, \tilde{T}_L) , $(\tilde{V}_R, \tilde{T}_L)$, and $(\tilde{V}_L, \tilde{T}_L)$ NP parameter space at 95% (blue) CL obtained from the measured values of R_D , R_{D^*} , and $R_{J/\Psi}$. We also show the allowed ranges in (R_D, P_τ^D) , $(R_{D^*}, P_\tau^{D^*})$, and $(R_{J/\Psi}, P_\tau^{J/\Psi})$ for each of these NP scenarios. It is clear that with all these NP couplings, the allowed ranges in R_D , R_{D^*} , $R_{J/\Psi}$, and $P_\tau^{D^*}$ at 95% (blue) CL do overlap with the experimentally allowed values within 1σ . It should, however, be mentioned that with $(\tilde{V}_R, \tilde{T}_L)$ NP couplings, the value of P_τ^D can be negative depending on the value of the NP couplings. Similarly, we do not see much variation of P_τ^D with (V_R, \tilde{T}_L) NP couplings. Measurement of P_τ^D and $P_\tau^{J/\Psi}$ in future will also play a crucial role.

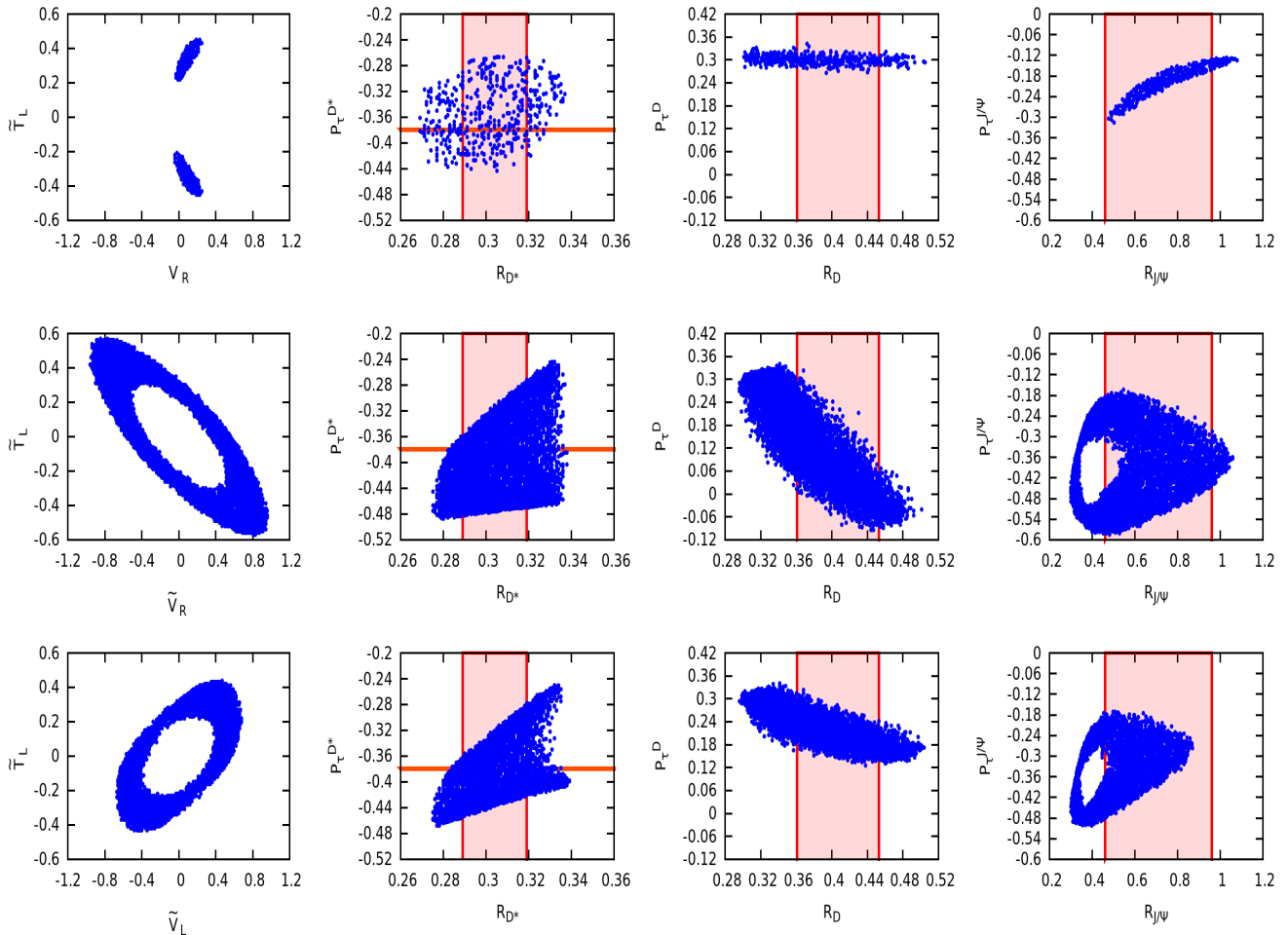


FIG. 2: The allowed NP parameter space (leftmost panels) at 95% (blue) CL from R_D , R_{D^*} , and $R_{J/\Psi}$ measurements. The corresponding allowed ranges in $(R_D, P_{\tau^D}^D)$, $(R_{D^*}, P_{\tau^{D^*}}^D)$, and $(R_{J/\Psi}, P_{\tau^{J/\Psi}}^D)$ are shown with blue dots. The experimental 1σ range of R_D , R_{D^*} , and $R_{J/\Psi}$ are shown with light red bands. The horizontal line in the second panel represents the central value of $P_{\tau^{D^*}}^D$ reported by BELLE.

IV. CONCLUSION

In view of the recent result of $R_{J/\Psi}$, we investigate R_D , R_{D^*} , and $R_{J/\Psi}$ anomalies using a model-independent framework. We consider total 55 NP models consisting of single as well as double NP coefficients and evaluate χ_{\min}^2 by including three measurements, namely, R_D , R_{D^*} , and $R_{J/\Psi}$. We find various NP models that can simultaneously explain R_D , R_{D^*} , and $R_{J/\Psi}$ anomalies within 1σ . We also give prediction on the τ polarization fraction parameter for all these decay modes in each NP scenarios. It should be noted that a more precise measurement on $P_{\tau^{D^*}}^D$ in future will be crucial to identify the true nature of NP. Again, in view of the immense importance of R_D , R_{D^*} , and $R_{J/\Psi}$, both experimentally and theoretically, it is important to ensure that theoretical calculations of various form factors are very precise. At the same time, measurement of $P_{\tau^D}^D$ and $P_{\tau^{J/\Psi}}^D$ in future will be crucial to rule out various NP scenarios.

[1] J. P. Lees *et al.* [BaBar Collaboration], “Evidence for an excess of $\bar{B} \rightarrow D^{(*)}\tau^-\bar{\nu}_\tau$ decays,” Phys. Rev. Lett. **109**, 101802 (2012) doi:10.1103/PhysRevLett.109.101802 [arXiv:1205.5442 [hep-ex]].

- [2] J. P. Lees *et al.* [BaBar Collaboration], “Measurement of an Excess of $\bar{B} \rightarrow D^{(*)}\tau^-\bar{\nu}_\tau$ Decays and Implications for Charged Higgs Bosons,” *Phys. Rev. D* **88**, no. 7, 072012 (2013) doi:10.1103/PhysRevD.88.072012 [arXiv:1303.0571 [hep-ex]].
- [3] M. Huschle *et al.* [Belle Collaboration], “Measurement of the branching ratio of $\bar{B} \rightarrow D^{(*)}\tau^-\bar{\nu}_\tau$ relative to $\bar{B} \rightarrow D^{(*)}\ell^-\bar{\nu}_\ell$ decays with hadronic tagging at Belle,” *Phys. Rev. D* **92**, no. 7, 072014 (2015) doi:10.1103/PhysRevD.92.072014 [arXiv:1507.03233 [hep-ex]].
- [4] Y. Sato *et al.* [Belle Collaboration], “Measurement of the branching ratio of $\bar{B}^0 \rightarrow D^{*+}\tau^-\bar{\nu}_\tau$ relative to $\bar{B}^0 \rightarrow D^{*+}\ell^-\bar{\nu}_\ell$ decays with a semileptonic tagging method,” *Phys. Rev. D* **94**, no. 7, 072007 (2016) doi:10.1103/PhysRevD.94.072007 [arXiv:1607.07923 [hep-ex]].
- [5] S. Hirose *et al.* [Belle Collaboration], “Measurement of the τ lepton polarization and $R(D^*)$ in the decay $\bar{B} \rightarrow D^*\tau^-\bar{\nu}_\tau$,” *Phys. Rev. Lett.* **118**, no. 21, 211801 (2017) doi:10.1103/PhysRevLett.118.211801 [arXiv:1612.00529 [hep-ex]].
- [6] R. Aaij *et al.* [LHCb Collaboration], “Measurement of the ratio of branching fractions $\mathcal{B}(\bar{B}^0 \rightarrow D^{*+}\tau^-\bar{\nu}_\tau)/\mathcal{B}(\bar{B}^0 \rightarrow D^{*+}\mu^-\bar{\nu}_\mu)$,” *Phys. Rev. Lett.* **115**, no. 11, 111803 (2015) Addendum: [*Phys. Rev. Lett.* **115**, no. 15, 159901 (2015)] doi:10.1103/PhysRevLett.115.159901, 10.1103/PhysRevLett.115.111803 [arXiv:1506.08614 [hep-ex]].
- [7] R. Aaij *et al.* [LHCb Collaboration], “Measurement of the ratio of the $B^0 \rightarrow D^{*-}\tau^+\nu_\tau$ and $B^0 \rightarrow D^{*-}\mu^+\nu_\mu$ branching fractions using three-prong τ -lepton decays,” arXiv:1708.08856 [hep-ex].
- [8] J. A. Bailey *et al.* [MILC Collaboration], “BD form factors at nonzero recoil and $-V_{cb}$ from 2+1-flavor lattice QCD,” *Phys. Rev. D* **92**, no. 3, 034506 (2015) doi:10.1103/PhysRevD.92.034506 [arXiv:1503.07237 [hep-lat]].
- [9] H. Na *et al.* [HPQCD Collaboration], “ $B \rightarrow D\ell\nu$ form factors at nonzero recoil and extraction of $|V_{cb}|$,” *Phys. Rev. D* **92**, no. 5, 054510 (2015) Erratum: [*Phys. Rev. D* **93**, no. 11, 119906 (2016)] doi:10.1103/PhysRevD.93.119906, 10.1103/PhysRevD.92.054510 [arXiv:1505.03925 [hep-lat]].
- [10] S. Aoki *et al.*, “Review of lattice results concerning low-energy particle physics,” *Eur. Phys. J. C* **77**, no. 2, 112 (2017) doi:10.1140/epjc/s10052-016-4509-7 [arXiv:1607.00299 [hep-lat]].
- [11] D. Bigi and P. Gambino, “Revisiting $B \rightarrow D\ell\nu$,” *Phys. Rev. D* **94**, no. 9, 094008 (2016) doi:10.1103/PhysRevD.94.094008 [arXiv:1606.08030 [hep-ph]].
- [12] S. Fajfer, J. F. Kamenik and I. Nisandzic, “On the $B \rightarrow D^*\tau\bar{\nu}_\tau$ Sensitivity to New Physics,” *Phys. Rev. D* **85**, 094025 (2012) doi:10.1103/PhysRevD.85.094025 [arXiv:1203.2654 [hep-ph]].
- [13] Y. Amhis *et al.*, “Averages of b -hadron, c -hadron, and τ -lepton properties as of summer 2016,” arXiv:1612.07233 [hep-ex].
- [14] LHCb-PAPER-2017-035.
- [15] Presentation by M. Fontana, on behalf of LHCb Collaboration.
- [16] W. F. Wang, Y. Y. Fan and Z. J. Xiao, “Semileptonic decays $B_c \rightarrow (\eta_c, J/\Psi)\ell\nu$ in the perturbative QCD approach,” *Chin. Phys. C* **37**, 093102 (2013) doi:10.1088/1674-1137/37/9/093102 [arXiv:1212.5903 [hep-ph]].
- [17] R. Dutta and A. Bhol, “ $B_c \rightarrow (J/\psi, \eta_c)\tau\nu$ semileptonic decays within the standard model and beyond,” *Phys. Rev. D* **96**, no. 7, 076001 (2017) doi:10.1103/PhysRevD.96.076001 [arXiv:1701.08598 [hep-ph]].
- [18] S. Fajfer, J. F. Kamenik, I. Nisandzic and J. Zupan, “Implications of Lepton Flavor Universality Violations in B Decays,” *Phys. Rev. Lett.* **109**, 161801 (2012) [arXiv:1206.1872 [hep-ph]].;
- [19] M. Tanaka, “Charged Higgs effects on exclusive semitauonic B decays,” *Z. Phys. C* **67**, 321 (1995) [hep-ph/9411405].;
- [20] U. Nierste, S. Trine and S. Westhoff, “Charged-Higgs effects in a new $B \rightarrow D\tau\nu$ differential decay distribution,” *Phys. Rev. D* **78**, 015006 (2008) [arXiv:0801.4938 [hep-ph]].;
- [21] T. Miki, T. Miura and M. Tanaka, “Effects of charged Higgs boson and QCD corrections in anti-B \rightarrow D tau anti-nu(tau),” hep-ph/0210051.;
- [22] A. Crivellin, C. Greub and A. Kokulu, “Explaining $B \rightarrow D\tau\nu$, $B \rightarrow D^*\tau\nu$ and $B \rightarrow \tau\nu$ in a 2HDM of type III,” *Phys. Rev. D* **86**, 054014 (2012) [arXiv:1206.2634 [hep-ph]].;
- [23] A. Datta, M. Duraisamy and D. Ghosh, “Diagnosing New Physics in $b \rightarrow c\tau\nu_\tau$ decays in the light of the recent BaBar result,” *Phys. Rev. D* **86**, 034027 (2012) [arXiv:1206.3760 [hep-ph]].;
- [24] M. Duraisamy and A. Datta, “The Full $B \rightarrow D^*\tau^-\bar{\nu}_\tau$ Angular Distribution and CP violating Triple Products,” *JHEP* **1309**, 059 (2013) [arXiv:1302.7031 [hep-ph]].
- [25] M. Duraisamy, P. Sharma and A. Datta, “Azimuthal $B \rightarrow D^*\tau^-\bar{\nu}_\tau$ angular distribution with tensor operators,” *Phys. Rev. D* **90**, no. 7, 074013 (2014) doi:10.1103/PhysRevD.90.074013 [arXiv:1405.3719 [hep-ph]].
- [26] P. Biancofiore, P. Colangelo and F. De Fazio, “On the anomalous enhancement observed in $B \rightarrow D^{(*)}\tau\bar{\nu}_\tau$ decays,” *Phys. Rev. D* **87**, 074010 (2013) [arXiv:1302.1042 [hep-ph]].;
- [27] A. Celis, M. Jung, X. -Q. Li and A. Pich, “Sensitivity to charged scalars in $B \rightarrow D^{(*)}\tau\nu_\tau$ and $B \rightarrow \tau\nu_\tau$ decays,” *JHEP* **1301**, 054 (2013) [arXiv:1210.8443 [hep-ph]].;
- [28] X. -G. He and G. Valencia, “B decays with τ -leptons in non-universal left-right models,” *Phys. Rev. D* **87**, 014014 (2013) [arXiv:1211.0348 [hep-ph]].;
- [29] R. Dutta, A. Bhol and A. K. Giri, “Effective theory approach to new physics in $b \rightarrow u$ and $b \rightarrow c$ leptonic and semileptonic decays,” *Phys. Rev. D* **88**, no. 11, 114023 (2013) doi:10.1103/PhysRevD.88.114023 [arXiv:1307.6653 [hep-ph]].
- [30] N. G. Deshpande and X. G. He, “Consequences of R-parity violating interactions for anomalies in $\bar{B} \rightarrow D^{(*)}\tau\bar{\nu}$ and $b \rightarrow s\mu^+\mu^-$,” *Eur. Phys. J. C* **77**, no. 2, 134 (2017) doi:10.1140/epjc/s10052-017-4707-y [arXiv:1608.04817 [hep-ph]].
- [31] X. Q. Li, Y. D. Yang and X. Zhang, “Revisiting the one leptoquark solution to the $R(D^{(*)})$ anomalies and its phenomenological implications,” *JHEP* **1608**, 054 (2016) doi:10.1007/JHEP08(2016)054 [arXiv:1605.09308 [hep-ph]].
- [32] D. Bardhan, P. Byakti and D. Ghosh, “A closer look at the R_D and R_{D^*} anomalies,” *JHEP* **1701**, 125 (2017) doi:10.1007/JHEP01(2017)125 [arXiv:1610.03038 [hep-ph]].
- [33] A. K. Alok, D. Kumar, S. Kumbhakar and S. U. Sankar, “ D^* polarization as a probe to discriminate new physics in

- $\bar{B} \rightarrow D^* \tau \bar{\nu}$,” Phys. Rev. D **95**, no. 11, 115038 (2017) doi:10.1103/PhysRevD.95.115038 [arXiv:1606.03164 [hep-ph]].
- [34] M. A. Ivanov, J. G. Körner and C. T. Tran, “Exclusive decays $B \rightarrow \ell^- \bar{\nu}$ and $B \rightarrow D^{(*)} \ell^- \bar{\nu}$ in the covariant quark model,” Phys. Rev. D **92**, no. 11, 114022 (2015) doi:10.1103/PhysRevD.92.114022 [arXiv:1508.02678 [hep-ph]].
- [35] M. A. Ivanov, J. G. Krner and C. T. Tran, “Analyzing new physics in the decays $\bar{B}^0 \rightarrow D^{(*)} \tau^- \bar{\nu}_\tau$ with form factors obtained from the covariant quark model,” Phys. Rev. D **94**, no. 9, 094028 (2016) doi:10.1103/PhysRevD.94.094028 [arXiv:1607.02932 [hep-ph]].
- [36] S. Nandi, S. K. Patra and A. Soni, “Correlating new physics signals in $B \rightarrow D^{(*)} \tau \nu_\tau$ with $B \rightarrow \tau \nu_\tau$,” arXiv:1605.07191 [hep-ph].
- [37] R. Dutta and A. Bhol, “ $b \rightarrow (c, s) \tau \nu$ leptonic and semileptonic decays within an effective field theory approach,” Phys. Rev. D **96**, no. 3, 036012 (2017) doi:10.1103/PhysRevD.96.036012 [arXiv:1611.00231 [hep-ph]].
- [38] R. Alonso, B. Grinstein and J. Martin Camalich, “Lifetime of B_c^- Constrains Explanations for Anomalies in $B \rightarrow D^{(*)} \tau \nu$,” Phys. Rev. Lett. **118**, no. 8, 081802 (2017) doi:10.1103/PhysRevLett.118.081802 [arXiv:1611.06676 [hep-ph]].
- [39] A. Celis, M. Jung, X. Q. Li and A. Pich, “Scalar contributions to $b \rightarrow c(u) \tau \nu$ transitions,” Phys. Lett. B **771**, 168 (2017) doi:10.1016/j.physletb.2017.05.037 [arXiv:1612.07757 [hep-ph]].
- [40] W. Altmannshofer, P. S. B. Dev and A. Soni, “ $R_{D^{(*)}}$ anomaly: A possible hint for natural supersymmetry with R -parity violation,” arXiv:1704.06659 [hep-ph].
- [41] S. Iguro and K. Tobe, “ $R(D^{(*)})$ in a general two Higgs doublet model,” arXiv:1708.06176 [hep-ph].
- [42] R. Watanabe, “New Physics effect on $B_c \rightarrow J/\psi \tau \bar{\nu}$ in relation to the $R_{D^{(*)}}$ anomaly,” arXiv:1709.08644 [hep-ph].
- [43] B. Chauhan and B. Kindra, “Invoking Chiral Vector Leptoquark to explain LFU violation in B Decays,” arXiv:1709.09989 [hep-ph].
- [44] I. I. Y. Bigi, “Inclusive B(c) decays as a QCD lab,” Phys. Lett. B **371**, 105 (1996) doi:10.1016/0370-2693(95)01574-4 [hep-ph/9510325].
- [45] M. Beneke and G. Buchalla, “The B_c Meson Lifetime,” Phys. Rev. D **53**, 4991 (1996) doi:10.1103/PhysRevD.53.4991 [hep-ph/9601249].
- [46] C. H. Chang, S. L. Chen, T. F. Feng and X. Q. Li, “The Lifetime of B_c meson and some relevant problems,” Phys. Rev. D **64**, 014003 (2001) doi:10.1103/PhysRevD.64.014003 [hep-ph/0007162].
- [47] A. G. Akeroyd and C. H. Chen, “Constraint on the branching ratio of $B_c \rightarrow \tau \bar{\nu}$ from LEP1 and consequences for $R(D^{(*)})$ anomaly,” Phys. Rev. D **96**, no. 7, 075011 (2017) doi:10.1103/PhysRevD.96.075011 [arXiv:1708.04072 [hep-ph]].
- [48] T. Bhattacharya, V. Cirigliano, S. D. Cohen, A. Filipuzzi, M. Gonzalez-Alonso, M. L. Graesser, R. Gupta and H. -W. Lin, “Probing Novel Scalar and Tensor Interactions from (Ultra)Cold Neutrons to the LHC,” Phys. Rev. D **85**, 054512 (2012) [arXiv:1110.6448 [hep-ph]].
- [49] V. Cirigliano, J. Jenkins and M. Gonzalez-Alonso, “Semileptonic decays of light quarks beyond the Standard Model,” Nucl. Phys. B **830**, 95 (2010) [arXiv:0908.1754 [hep-ph]].
- [50] C. Patrignani *et al.* [Particle Data Group], “Review of Particle Physics,” Chin. Phys. C **40**, no. 10, 100001 (2016). doi:10.1088/1674-1137/40/10/100001
- [51] B. Colquhoun *et al.* [HPQCD Collaboration], “B-meson decay constants: a more complete picture from full lattice QCD,” Phys. Rev. D **91**, no. 11, 114509 (2015) doi:10.1103/PhysRevD.91.114509 [arXiv:1503.05762 [hep-lat]].
- [52] A. Lytle, B. Colquhoun, C. Davies, J. Koponen and C. McNeile, “Semileptonic B_c decays from full lattice QCD,” PoS BEAUTY **2016**, 069 (2016) [arXiv:1605.05645 [hep-lat]].
- [53] B. Colquhoun *et al.* [HPQCD Collaboration], “ B_c decays from highly improved staggered quarks and NRQCD,” PoS LATTICE **2016**, 281 (2016) [arXiv:1611.01987 [hep-lat]].
- [54] D. Melikhov and B. Stech, “Weak form-factors for heavy meson decays: An Update,” Phys. Rev. D **62**, 014006 (2000) doi:10.1103/PhysRevD.62.014006 [hep-ph/0001113].
- [55] I. Caprini, L. Lellouch and M. Neubert, “Dispersive bounds on the shape of anti-B \rightarrow $D^{(*)}$ lepton anti-neutrino form-factors,” Nucl. Phys. B **530**, 153 (1998) doi:10.1016/S0550-3213(98)00350-2 [hep-ph/9712417].

Coefficients	Best fit value	R_D	R_{D^*}	$R_{J/\psi}$	$P_\tau^{D^*}$	$\mathcal{B}(B_c \rightarrow \tau\nu)\%$	χ_{\min}^2
(V_L, V_R)	(-2.14, -0.04)	0.406	0.308	0.357	-0.500	2.7	2.1
(V_L, S_L)	(-1.94, 1.62)	0.403	0.308	0.383	-0.092	137.3	1.8
(V_L, S_R)	(0.09, 0.13)	0.411	0.305	0.352	-0.475	6.3	2.1
(V_L, T_L)	(-2.13, -0.03)	0.404	0.302	0.320	-0.502	2.8	2.5
(V_L, \tilde{V}_L)	(-1.68, -0.87)	0.397	0.306	0.356	0.121	2.7	2.1
(V_L, \tilde{V}_R)	(-1.68, -0.87)	0.397	0.306	0.356	0.121	2.7	2.1
(V_L, \tilde{S}_L)	(-2.10, -0.29)	0.403	0.305	0.353	-0.498	5.9	2.1
(V_L, \tilde{S}_R)	(-2.10, -0.29)	0.403	0.305	0.353	-0.498	5.9	2.1
(V_L, \tilde{T}_L)	(0.04, -0.23)	0.361	0.312	0.534	-0.439	2.3	1.8
(V_R, S_L)	(0.08, -1.68)	0.406	0.307	0.372	-0.070	154.1	1.9
(V_R, S_R)	(-0.09, 0.27)	0.402	0.306	0.359	-0.445	10.5	2.1
(V_R, T_L)	(0.25, -0.27)	0.399	0.304	0.822	-0.365	1.2	0.24
(V_R, \tilde{V}_L)	(0.06, 0.56)	0.408	0.303	0.355	-0.238	2.6	2.1
(V_R, \tilde{V}_R)	(0.06, 0.56)	0.408	0.303	0.355	-0.238	2.6	2.1
(V_R, \tilde{S}_L)	(-0.10, 0.72)	0.410	0.306	0.359	-0.507	22.9	2.0
(V_R, \tilde{S}_R)	(-0.10, 0.72)	0.410	0.306	0.359	-0.507	22.9	2.0
$(\mathbf{V}_R, \tilde{\mathbf{T}}_L)$	(0.08, 0.33)	0.405	0.304	0.722	-0.365	1.9	0.43×10^{-2}
(S_L, S_R)	(-0.49, 0.71)	0.405	0.309	0.386	-0.224	79.9	1.8
(S_L, T_L)	(0.20, -0.10)	0.413	0.303	0.512	-0.486	0.04	0.66
(S_L, \tilde{V}_L)	(0.06, -0.47)	0.400	0.305	0.358	-0.326	1.5	2.0
(S_L, \tilde{V}_R)	(0.06, -0.47)	0.400	0.305	0.358	-0.326	1.5	2.0
(S_L, \tilde{S}_L)	(-1.08, -0.86)	0.407	0.311	0.393	-0.271	109.1	1.8
(S_L, \tilde{S}_R)	(-1.08, -0.86)	0.407	0.311	0.393	-0.271	109.1	1.8
(S_L, \tilde{T}_L)	(0.18, -0.28)	0.410	0.305	0.629	-0.429	0.10	0.12
(S_R, T_L)	(-1.66, -0.12)	0.421	0.307	0.548	-0.544	91.2	0.57
(S_R, \tilde{V}_L)	(0.14, -0.44)	0.404	0.305	0.360	-0.317	6.4	2.0
(S_R, \tilde{V}_R)	(0.14, -0.44)	0.404	0.305	0.360	-0.317	6.4	2.0
(S_R, \tilde{S}_L)	(0.30, 0.10)	0.438	0.266	0.307	-0.438	12.7	9.8
(S_R, \tilde{S}_R)	(0.30, 0.10)	0.438	0.266	0.307	-0.438	12.7	9.8
(S_R, \tilde{T}_L)	(-1.63, -0.31)	0.405	0.305	0.676	-0.481	80.5	0.26×10^{-1}
(T_L, \tilde{V}_L)	(0.01, 0.48)	0.394	0.308	0.345	-0.310	2.5	2.3
(T_L, \tilde{V}_R)	(0.01, 0.48)	0.394	0.308	0.345	-0.310	2.5	2.3
(T_L, \tilde{S}_L)	(-0.08, -0.66)	0.405	0.302	0.472	-0.473	18.1	0.94
(T_L, \tilde{S}_R)	(-0.08, -0.66)	0.405	0.302	0.472	-0.473	18.1	0.94
(T_L, \tilde{T}_L)	(0.12, -0.38)	0.392	0.307	0.741	-0.345	2.3	0.16
$(\tilde{V}_L, \tilde{V}_R)$	(-0.05, -0.52)	0.413	0.308	0.362	-0.313	2.5	2.1
$(\tilde{V}_L, \tilde{S}_L)$	(0.37, -0.80)	0.412	0.306	0.364	-0.415	34.2	2.0
$(\tilde{V}_L, \tilde{S}_R)$	(0.44, 0.15)	0.405	0.304	0.358	-0.342	4.9	2.0
$(\tilde{\mathbf{V}}_L, \tilde{\mathbf{T}}_L)$	(-0.34, -0.35)	0.405	0.306	0.635	-0.427	2.6	0.11
$(\tilde{V}_R, \tilde{S}_L)$	(0.44, 0.15)	0.405	0.304	0.358	-0.342	4.9	2.0
$(\tilde{V}_R, \tilde{S}_R)$	(0.37, -0.80)	0.412	0.306	0.364	-0.415	34.2	2.0
$(\tilde{\mathbf{V}}_R, \tilde{\mathbf{T}}_L)$	(-0.68, 0.44)	0.405	0.304	0.686	-0.446	3.1	0.13×10^{-1}
$(\tilde{S}_L, \tilde{S}_R)$	(1.36, -0.73)	0.405	0.305	0.374	-0.586	206.5	1.9
$(\tilde{S}_L, \tilde{T}_L)$	(0.49, -0.27)	0.399	0.307	0.619	-0.418	12.1	0.22
$(\tilde{S}_R, \tilde{T}_L)$	(0.49, -0.27)	0.399	0.307	0.619	-0.418	12.1	0.22

TABLE II: Best estimates of R_D , R_{D^*} , $R_{J/\psi}$, $P_\tau^{D^*}$, and $\mathcal{B}(B_c \rightarrow \tau\nu)$ within various NP scenarios.